Iraqi Journal of Science
ISSN: 0067-2904

Elastic electron scattering from ^{6}He and ^{11}Li halo nuclei

Ahmed N. Abdullah
Department of Physics, College of Science, University of Baghdad, Baghdad, Iraq

Abstract

The binary cluster model (BCM) and the two-frequency shell model (TFSM) have been used to study the ground state matter densities of neutron-rich ^{6}He and ^{11}Li halo nuclei. Calculations show that both models provide a good description on the matter density distribution of above nuclei. The root-mean square (rms) proton, neutron and matter radii of these halo nuclei obtained by TFSM have been successfully obtained. The elastic charge form factors for these halo nuclei are studied through combining the charge density distribution obtained by TFSM with the plane wave Born approximation (PWBA).

Keywords: neutron-rich halo nuclei; binary cluster model.

الاستطارة الالكترونية المرنة من نوى الهالة ^{6}He و ^{11}Li

أحمد نجم عبدالله
قسم الفيزياء ، كلية العلوم، جامعة بغداد، بغداد، العراق

الخلاصة

تم استخدام الانموذج العنقودي الثنائي (BCM) و أنموذج القشرة ذو الترددين (TFSM) لدراسة توزيعات الكثافة المادية لنوى الهالة والغنية بالنيوترونات ^{6}He و ^{11}Li. ان الحسابات اظهرت ان كل من النموذجين يعطي نتائج جيدة بالنسبة لتوزيعات الكثافة المادية. ان حسابات انصاف الاقطار البروتونية والنيوترونية والكتلية باستخدام أنموذج القشرة ذو الترددين (TFSM) لهذه النوى تتفق بشكل جيد مع القيم العملية. ان عوامل التشكل المرنة لهذه النوى تم دراستها بواسطة تقريب بورن للموجة المستوية مع استخدام توزيع الكثافة الشحنية التي تم الحصول عليها من خلال أنموذج القشرة ذو الترددين (TFSM).

1. Introduction

Since the discoveries of neutron halo in exotic light neutron-rich nuclei in the mid-eighties [1-3], studies on halo phenomena have become a hot point in nuclear physics. The cause of halo phenomena lies in both the small separation energy of the last few nucleons and their occupation on the orbits with low angular momentum (l = 0, 1) [4], which allow the wave function of the valence nucleons to extend to large radii [5]. The observation of large total interaction cross sections for ^{11}Li, ^{11}Be, and ^{14}Be by Tanihata *et al*. showed that halo is probably present in many neutron-rich nuclei close to the drip line and initialized intensive experimental and theoretical work on neutron-rich nuclei [1]. Such a behavior shows up also on the proton-rich side of the chart of nuclei. But the study of proton-rich nuclei is scarce as compared with that of neutron-rich nuclei. It is believed that it is slightly hard for proton-rich nuclei to form the halo structure because of Coulomb barrier, which hinder the proton to penetrate into the out region of the nuclear-core [5, 6].

*Email: Ahmednajim@scbaghdad.edu.iq

The halo nuclei have large neutron excess or proton excess where a few outside nucleons are very weakly bound. Such halo systems are well described by the few body models, which assume that halo nuclei consist of a tightly bound inner core surrounded by a few outer nucleons that are loosely bound to it [7]. So the halo nuclei can be divided into two types: the two-body halo where one nucleon is surrounding the core nucleus, such as the one-neutron halo ^{11}Be and the one-proton halo ^{8}B; and the three-body halo where two valence nucleons are around the core nucleus, such as ^{6}He and ^{11}Li [8]. The three-body halo have been called Borromean because where the two-body subsystems (core plus one neutron or the di-neutron) are unbound, but the three-body system is bound [9, 10].

Abdullah [11] has been used the single-particle radial wave functions of Woods-Saxon (WS) potential within the three-body model of $(Core + n + n)$ to study the ground state densities and the associated root mean square (rms) radii of some two neutrons halo nuclei (such as ^{6}He, ^{11}Li, ^{12}Be and ^{14}Be). The halo structure of selected halo nuclei was emphasized through exhibiting the long tail performance in their calculated neutron and matter density distributions, where this performance is considered as a distinctive feature of halo nuclei. The elastic electron scattering form factors for these nuclei were studied via the plane wave Born approximation.

Abdullah [12] has been used the MSK7 Skyrme parameter within the Skyrme-Hartree-Fock (SHF) method to study the ground state densities, the associated rms radii and the binding energy per nucleon of two neutrons ^{6}He, ^{11}Li, ^{12}Be and ^{14}Be halo nuclei. He found that the calculated results are in an excellent accordance with those of experimental data. The elastic electron scattering form factors for these nuclei were studied by the plane wave Born approximation.

2. Theory

The ground state densities of halo nuclei are calculated by two distinct models, these are the binary cluster model (BCM) and the two frequency shell model (TFSM).

In BCM [13], the halo nucleus is assumed as composite projectile of mass A_p consisting of core and valence clusters, of masses A_c and A_v bounded with a state of relative motion (Figure-1). The matter density of the composite projectile is given by [13]

$$\rho_m(r) = A_c\, g^{(3)}(\hat{\alpha}_c, r) + A_v\, g^{(3)}(\hat{\alpha}_v, r) \tag{1}$$

Where $g^{(3)}$ is the normalized 3-dimensional Gaussian function

$$g^{(3)}\left(\hat{\alpha}_{c(v)}, r\right) = \frac{1}{\pi^{3/2}\hat{\alpha}_{c(v)}^{3}}\, e^{-r^2/\hat{\alpha}_{c(v)}^{2}}, \qquad \int g^{(3)}\left(\alpha_{c(v)}, r\right) d\vec{r} = 1 \tag{2}$$

with range parameters

$$\hat{\alpha}_c{}^2 = \alpha_c{}^2 + \left(\frac{A_v \alpha}{A_v + A_c}\right)^2, \qquad \hat{\alpha}_v{}^2 = \alpha_v{}^2 + \left(\frac{A_c \alpha}{A_v + A_c}\right)^2 \tag{3}$$

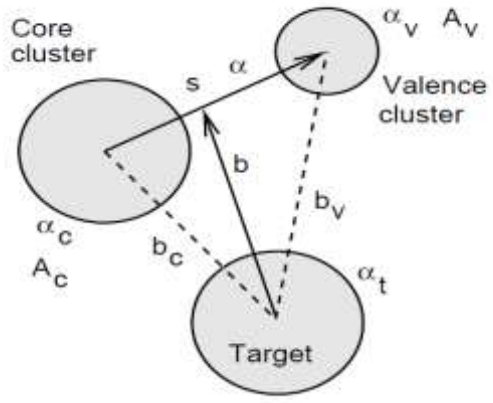

Figure 1-The two-cluster projectile and target coordinates.

In TFSM [14], the harmonic oscillator wave functions (HO) are used with two different oscillator size parameters b_c (for core nucleons) and b_v (for halo nucleons). This approach permits to work freely on each part by changing $b_{c(v)}$ till obtaining a fit with observed data. Therefore, the ground state matter density distribution separate into two parts [14]:

$$\rho_m(r) = \rho_c(r) + \rho_v(r), \quad (4)$$

where $\rho_c(r)$ and $\rho_v(r)$ are the core density and valence (halo) density, respectively. Moreover, the matter density of Eq. (4) can be expressed as [11,12]:

$$\rho_m(r) = \rho^p(r) + \rho^n(r), \quad (5)$$

where $\rho^p(r)$ and $\rho^n(r)$ are the proton density and neutron density, respectively expressed as [11,12]:

$$\rho^p(r) = \rho_c^p(r) + \rho_v^p(r) \quad (6)$$

and

$$\rho^n(r) = \rho_c^n(r) + \rho_v^n(r) \quad (7)$$

The normalization conditions for the ground state densities given in Eqs. (4-7) are [14]

$$g = 4\pi \int_0^\infty \rho_g(r)\, r^2\, dr, \quad (8)$$

and the corresponding rms radii are [14]

$$\langle r^2 \rangle_g^{1/2} = \frac{4\pi}{g} \int_0^\infty \rho_g(r) r^4 dr, \quad (9)$$

where $\rho_g(r)$ corresponds to the one of the densities $[\rho_m(r), \rho_c(r),\ \rho_v(r), \rho^p(r), \rho^n(r)\ ]$ and g corresponds to the number of nucleon in each case.

The elastic electron scattering form factors from considered nuclei are studied by the plane wave Born approximation (PWBA). The total charge form factor squared is given by [11, 12]:

$$|F_{ch}(q)|^2 = |F_0(q)|^2 + |F_2(q)|^2, \quad (10)$$

where $F_0(q)$ is the elastic charge form factor which given by the Fourier transform of the ground state charge density distribution obtained by TFSM [11,12]:

$$F_0(q) = \frac{4\pi}{Z} \int_0^\infty \rho_{0ch}(r) j_0(qr) r^2 dr, \quad (11)$$

where$j_0(qr)$ is the spherical Bessel function of order zero and q is the momentum transfer from the incident electron to the target nucleus. Inclusion the corrections of the finite nucleon size $F_{fs}(q) = exp(-0.43q^2/4)$ and the center of mass $F_{cm}(q) = exp(b^2q^2/4A)$ in the calculations needs multiplying the form factors of Eq. (11) by these corrections.

The quadrupole form factor, $F_2(q)$, is obtained by the undeformed p-shell model as [11, 12]:

$$F_2(q) = \frac{\langle r^2 \rangle}{Q} \left(\frac{4}{5P_J} \right)^{1/2} \int \rho_{2ch}(r) j_2(qr) r^2 dr \quad (12)$$

where $j_2(qr)$ is the second order of the spherical Bessel functions, Q is the quadrupole moment and P_J is a quadrupole projection factor given as [11,12]:

$$P_J = \frac{J(2J-1)}{(J+1)(2J+3)} \quad (13)$$

3. Results and discussion

The binary cluster model (BCM) and the two-frequency shell model (TFSM) have been used to study the ground state proton, neutron and matter densities of neutron-rich ^{6}He ($\tau_{1/2}$=806 ms, S_{2n}=0.975 MeV) and ^{11}Li ($\tau_{1/2}$=8.75 ms, S_{2n}=369 KeV) halo nuclei. The elastic charge form factors for these nuclei are studied through combining the charge density distribution obtained by TFSM with the plane wave Born approximation (PWBA). The ^{6}He and ^{11}Li are two-neutron Borromean halo nuclei composed of the core ^{4}He and ^{9}Li plus the valence (halo) two neutrons, respectively. The configurations $\{(1s_{1/2})^4\}$, and $\{(1s_{1/2})^4, (1p_{3/2})^5\}$ are assumed for core nuclei ^{4}He and ^{9}Li, respectively. The two valence neutrons in ^{6}He and ^{11}Li are assumed to be in a pure $1p_{1/2}$ orbit. The calculated core, matter, proton and neutron rms radii for selected halo nuclei using values of the harmonic oscillator size parameter $\left(b_c^p, b_c^n\ and\ b_v^n\right)$ along with the experimental data [15-18] are displayed in Tables-(1, 2). It is obvious from these tables that the calculated results are in an excellent accordance with those of experimental data.

Table 1-The calculated and experimental core and matter rms radii of ^{6}He and ^{11}Li halo nuclei along with parameters for $\left(b_c^p, b_c^n \text{ and } b_v^n\right)$ utilized in the TFSM.

Halo nuclei	Core nuclei	b_c^p (fm)	b_c^n (fm)	b_v^n (fm)	$\langle r_{core}^2\rangle_{cal}^{1/2}$ (fm)	$\langle r_{core}^2\rangle_{exp}^{1/2}$ [15]	$\langle r_m^2\rangle_{cal}^{1/2}$ (fm)	$\langle r_m^2\rangle_{exp}^{1/2}$ [16,17]
^{6}He	^{4}He	1.544	1.544	1.984	1.89	1.88±0.12	2.37	2.33±0.04
^{11}Li	^{9}Li	1.755	1.78	3.92	2.54	2.54±0.04	3.5	3.5±0.09

Table 2-The calculated proton and neutron rms radii along with the experimental results.

Nuclei	$\langle r_p^2\rangle_{cal}^{1/2}$	$\langle r_p^2\rangle_{exp}^{1/2}$ [17]	$\langle r_n^2\rangle_{cal}^{1/2}$	$\langle r_n^2\rangle_{exp}^{1/2}$ [17,18]	$\langle r_n^2\rangle^{1/2} - \langle r_p^2\rangle^{1/2}$
^{6}He	1.89	1.89±0.04	2.59	2.59±0.04	0.7
^{11}Li	2.37	2.37±0.04	3.84	3.84±0.11	1.46

Figure-2 demonstrates the calculated core, halo and matter density distributions of ^{6}He (top panel) and ^{11}Li (bottom panel) displayed as dashed, dash-dotted and solid curves, respectively. These distributions are obtained by the BCM [Figures-2(a) and 2(c)] and TFSM [Figures-2(b) and 2(d)]. For comparison we present the experimental matter densities (denoted by the grey area) of ^{6}He [17] and ^{11}Li [16]. One can see from figure 2 that the solid distributions describe the experimental data well in the whole range of *r*. Moreover, the dash-dotted and solid distributions show characteristic behavior of a halo structure (*i.e.*, a long tail manner) for selected nuclei.

Figure-3 illustrates the calculated proton and neutron density distributions displayed as dashed and dash-dotted curves, respectively. These distributions are calculated by the BCM [Figures. 3(a) and 3(c)] and TFSM [Figures-3(b) and 3(d)]. The long tail performance is clearly noticed in the dash-dotted curves. This performance is related to the existence of the valence two neutrons in the halo orbits. The steep slope performance is obviously observed in the dashed curves due to the absence of protons in the halo orbit, where all protons of these nuclei are found in its core only. The difference between the calculated neutron and proton rms radii is $R_n - R_p = 2.59 - 1.89 = 0.7$ fm for ^{6}He and $R_n - R_p = 3.84 - 2.37 = 1.46$ fm for ^{11}Li. This difference also gives a supplementary support for the halo structure of these nuclei.

Figure-4 exhibits the comparison between the calculated matter density distribution of unstable nuclei ^{6}He and ^{11}Li (dashed curves) and those of their stable isotopes ^{4}He and ^{7}Li (solid curves). The calculated densities in Figures 4(a) and 4(c) [obtained by BCM] are compared with corresponding densities in Figures 4(b) and 4(d) [obtained by TFSM]. It is clear from these figures that the dashed and solid curves are diverse. As the valence two neutrons in ^{6}He [^{11}Li] are weakly bounded, the dashed curve has a longer tail than that of the solid curve.

Figure-5 (a) exemplifies the comparison between the calculated elastic C0 charge form factors of unstable nucleus ^{6}He (solid curve) and that of stable nucleus ^{4}He (dashed curve). In this figure the dotted symbols refer to the experimental data of ^{4}He [19]. One can see from this figure that the solid and dashed curves have no diffraction minimum throughout all considered range of momentum transfer. Moreover, the form factor of ^{6}He decrease with momentum transfer where the addition of neutrons to ^{6}He pull the charge density out. The form factor is not dependent on detailed properties of the neutron halo. It is only the presence of the extra 2 neutrons that causes the change to the proton distribution. Figure-5 (b) exhibits the comparison between the calculated charge form factors (C0+C2) of nuclei ^{11}Li and ^{7}Li displayed as solid and dashed curves, respectively, while the dotted symbols refer to the experimental data of ^{7}Li [20]. The quadrupole form factors are calculated by Eq. (12) using $Q = 4.5$ and $\langle r^2\rangle^{1/2} = 3.5$ fm for ^{11}Li and $Q = 2.8$ and $\langle r^2\rangle^{1/2} = 2.33$ fm for ^{7}Li. One can see from this figure that the form factor of ^{11}Li decreases faster than that of ^{7}Li with increasing momentum transfer. As with ^{6}He, this is due only to the coupling of the 4 extra neutrons to the ^{7}Li core.

4. Conclusions

The ground state proton, neutron and matter densities of neutron-rich ^{6}He and ^{11}Li halo nuclei have been calculated in the framework of the binary cluster model (BCM) and the two-frequency shell model (TFSM). It is shown that both models work well for these neutron-rich halo nuclei. The halo structure of selected halo nuclei is emphasized through exhibiting the long tail performance in their calculated neutron and matter density distributions, where this performance is considered as a

distinctive feature of halo nuclei. A supplementary support for the halo structure of these halo nuclei is found due to the noticeable difference between the calculated overall proton and neutron root mean square radii. This study confirms that the structure of the two halo (valence) neutrons in ^{6}He and ^{11}Li are in a pure $1p_{1/2}$ orbit. The elastic electron scattering form factors for these nuclei are studied via the plane wave Born approximation. It found that the major difference between the charge form factors of the unstable nuclei and that of their stable isotopes is caused by the addition of neutrons to the stable isotopes which lead to extend the charge density of unstable nuclei.

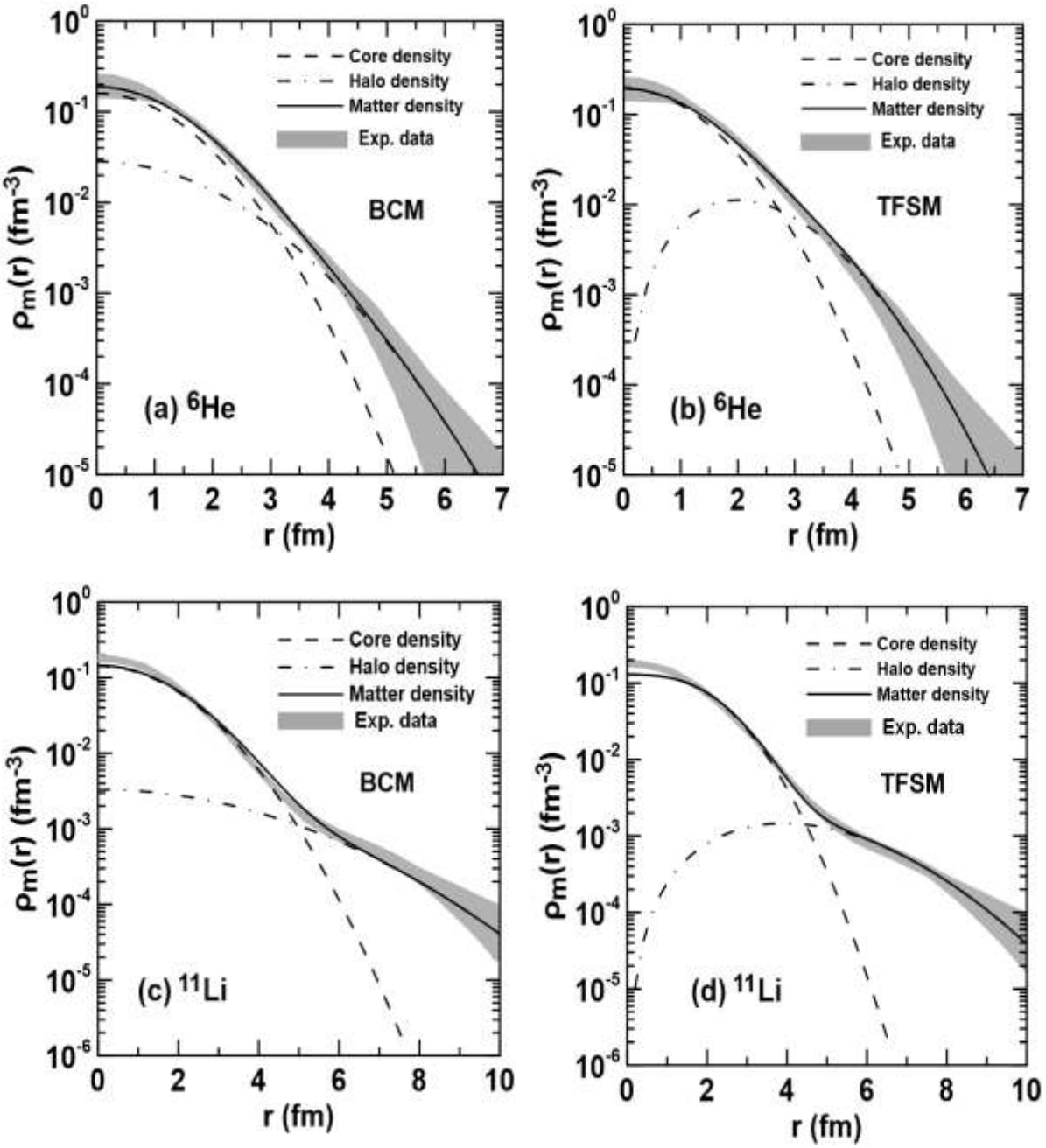

Figure 2-Matter density distributions for halo nuclei ^{6}He [Figures- (a) and (b)] and ^{11}Li [Figures-(c) and (d)]

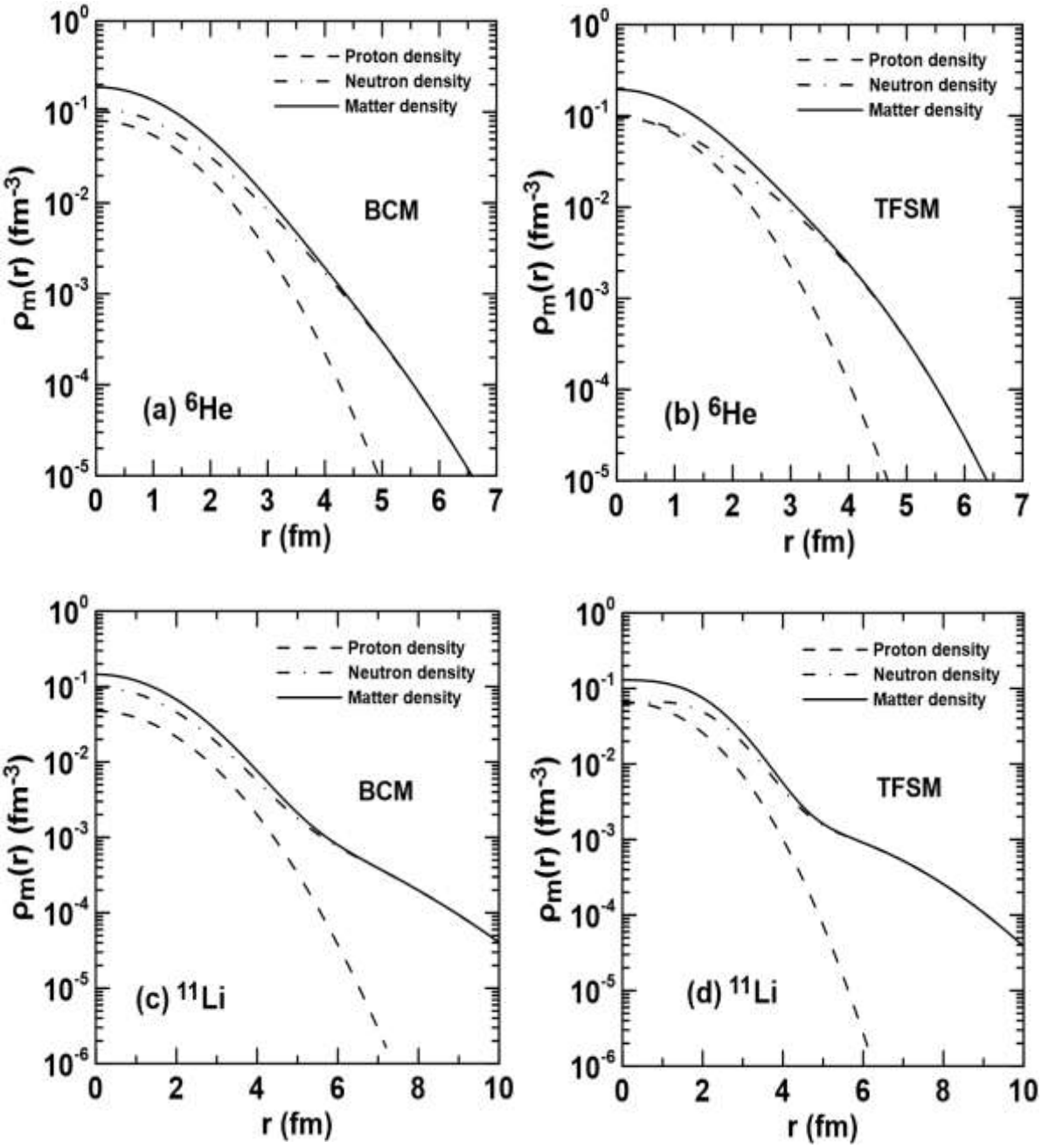

Figure 3-Neutron, proton and matter density distributions for halo nuclei ^{6}He [Figures-(a) and (b)] and ^{11}Li [Figures-(c) and (d)] calculated by the BCM and TFSM.

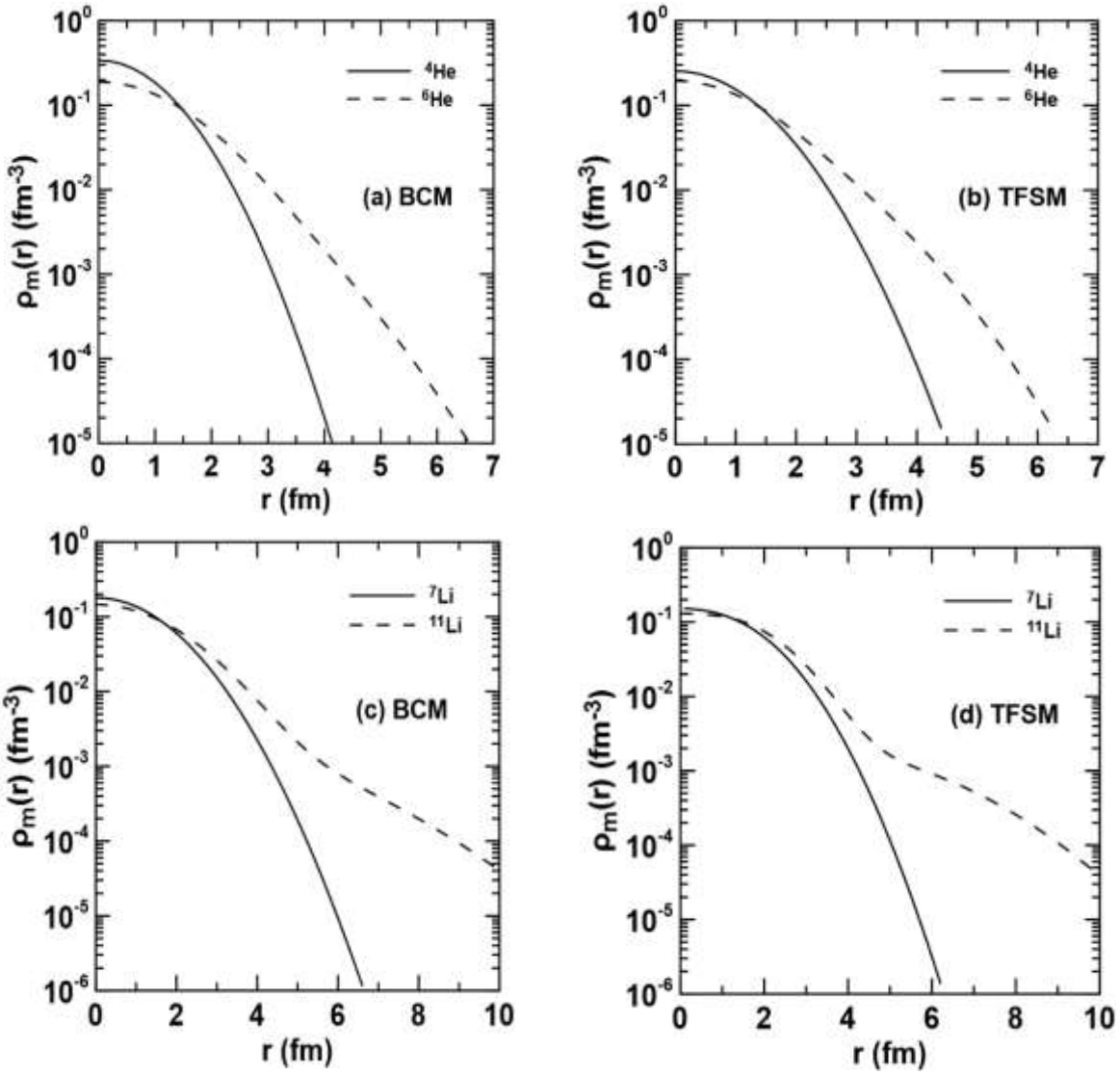

Figure 4-The calculated matter density of unstable nuclei (^{6}He, ^{11}Li) compared with those of their stable isotopes (^{4}He, ^{7}Li) obtained by the BCM and TFSM.

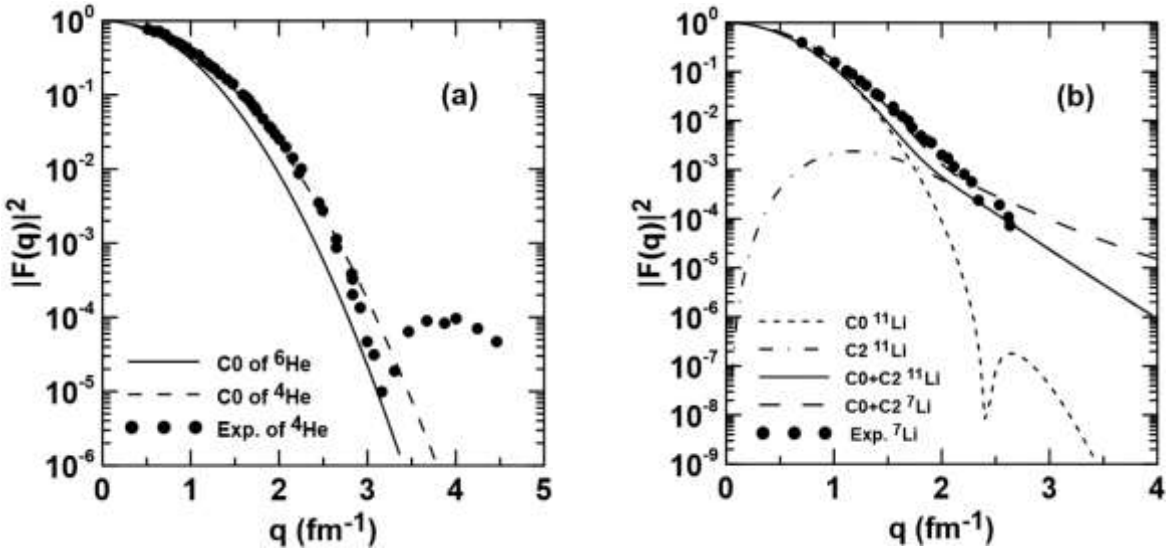

Figure 5-The charge form factors of unstable (halo) nuclei (^{6}He, ^{11}Li) compared with those of their stable isotopes (^{4}He, ^{7}Li).

References

1. Tanihata, I., Hamagaki, H., Hashimoto, O., Shida, Y., Yoshikawa, N., Sugimoto, K., Yamakawa, O. and Kobayashi, T. **1985**. Measurement of interaction cross sections and nuclear radii in the light p shell region. *Physical Review Letters*, **55**(24): 2676-2679.
2. Tanihata I., Hamagaki H., Hashimoto O., Nagamiya S., Shida Y., Yoshikawa N., Yamakawa O., Sugimoto K., Kobayashi T., Greiner D. E., Takahashi N. and Nojiri Y. **1985.** Measurement of interaction cross sections and radii of He isotopes. *Physics Letters* B, **160**(6): 380-384.
3. Hansen, P. G. and Jonson, B. **1987**. The neutron halo of extremely neutron-rich nuclei. *EurophysicsLetters*, **4**(4): 409-414.
4. Zaijun, W. and Zhongzhou, R. **2004**. Probing proton halo of the exotic nucleus ^{28}S by elastic electron scattering. *Science in China Series G Physics and Astronomy*, **47**: 42-51.
5. Blank, B., Marchand, C., Pravikoff, M.S., Baumann, T., Bou, F., Geissel, H., Hellström, M., Iwasa, N., Schwab, W., Sammerer, K. and Gai M. **1997**. Total interaction and proton-removal cross-section measurements for the proton-rich isotopes ^{7}Be, ^{8}B and ^{9}C. *Nuclear Physics* A **624**: 242-256.
6. Zhang, H.Y., Shen, W.Q., Ren, Z.Z., Ma, Y.G., Jiang, W.Z., Zhu, Z.Y., Cai, X.Z., Fang, D.Q., Zhong, C., Yu, L.P., Wei, Y.B., Zhan, W.L., Guo, Z.Y., Xiao, G.Q., Wang J.S., Wang J.C., Wang, Q.J., Li, J.X., Wang, M. and Chen Z.Q. **2002**. Measurement of reaction cross section for proton-rich nuclei (A<30) at intermediate energies. *Nuclear Physics* A **707**: 303-324.
7. Guo W. J., Jiang H. Q., Liu J. Y., Zuo W., Ren Z. Z. and Lee X. G. **2003**. Total nuclear reaction cross section induced by halo nuclei and stable nuclei. *Commun. Theoretical Physics*. (Beijing, China) **40**: 577-584.
8. Hu Z., Wang M., Xu H., Sun Z., Wang J., Xiao G., Zhan W., Xiao Z., Mao R.,2, Li C., Zhang X., Zhang H., Zhao T., Xu Z., Wang Y., Chen R., Huang T., Fu F., Gao Q., Han J., Zhang X., Zheng C., Yu Y. and Guo Z. **2008**. The properties of halo structure for ^{17}B. *Science in China Series G: Physics, Mechanics & Astronomy* **51**(7), pp: 781-787.
9. Vaagen, J. S., Gridne, D. K., Andersen H. H., Danilin, B. V., Ershov, S. N., Zagrebaev V. I., Thompson, I. J., Zhukov, M. V. and Bang, J. M. **2000**. Borromean halo nuclei. *Physica Scripta* T **88**: 209-213.
10. Zukov M. V., Danilin B. V., Fedorov D. V., Bang J. M., Thompson I. J. and Vaagen J. S.**1993**. Bound state properties of Borromean halo nuclei: ^{6}He and ^{11}Li. *Physics Reports* **231**(4):151-199.
11. Abdullah, A. N. **2017**. Nuclear structure investigation of some neutron-rich halo nuclei. *International Journal of Modern Physics* E **26**(7): 1-11.
12. Abdullah, A. N. **2017**. Matter density distributions and elastic form factors of some two-neutron halo nuclei. *Pramana Journal of Physics* **89**(43): 1-6.
13. Tostevin J. A., Johnson R. C. and Al-Khalili J. S.**1998**. Manifestation of halo size in scattering and reactions. *Nuclear Physics* A **630**, pp: 340c-351c.
14. Hamoudi, A. K., Flaiyh, G. N. and Abdullah, A. N. **2014**. Study of Matter Density Distributions, Elastic Electron Scattering form Factors and Reaction Cross Sections of ^{8}He and ^{17}B Exotic Nuclei. *Iraqi Journal of Science* **55** (4B): 1876-1890.
15. Alkhazov G.D., Dobrovolsky A.V. and Lobodenko A.A. **2004**. Matter density distributions and radii of light exotic nuclei from intermediate-energy proton elastic scattering and from interaction cross sections. *Nuclear Physics* A **734**: 361-364.
16. Antonov A. N., Kadrev D. N., Gaidarov M. K., Moya de Guerra E., Sarriguren P., Udias J. M., Lukyanov V. K., Zemlyanaya E. V., and Krumova G. Z. **2005**. Charge and matter distributions and form factors of light, medium, and heavy neutron-rich nuclei. *Physical Review* C **72**: 1-11.
17. Tanihata, I., Savajols, H., and Kanungo, R. **2013**. Recent experimental progress in nuclear halo structure studies. *Progress in Particle and Nuclear Physics* **68**: 215-313.
18. Tanihata, I., Hirata, D., Kobayashi, T., Shirnoura, S. 2, Sugimoto K. and Toki, H. **1992**. Revelation of thick neutron skins in nuclei. *Physics Letters* B **289**: 261-266.
19. McCarthy, J. S., Sick, I. and Whitney, R. R. **1977**. Electromagnetic structure of the helium isotopes, *Physical Review* C **15**: 1396-1414.
20. Suelzle L. R., Yearian M. R. and Crannell H. **1967**. Elastic electron scattering from ^{6}Li and ^{7}Li. *Physical Review* **162**: 992-1005.